JMEMS Letters

A Bistable Electrostatic Silicon Nanofin Relay for Nonvolatile Memory Application

Bowoon Soon, Eldwin Jiaqiang Ng, Navab Singh, Julius Minglin Tsai, You Qian, and Chengkuo Lee

***Abstract*—We present a nanoelectromechanical (NEM) relay that is capable of demonstrating two stable states without on-hold power due to the influence of van der Waals force. This is realized by leveraging a silicon nanofin (SiNF) as a relay that can switch between two lateral terminals. The smallest dimension of the SiNF is 80-nm width by 2-μm length. The SiNF is able to maintain its geometrical position even after the bias voltage is turned off. Bistable hysteresis behavior with pull-in voltage (V_{PI}) and reset voltage (V_{RESET}) as low as 8.4 and 10.1 V is measured. The nanoscale footprint of this device shows great potential for high-density nonvolatile memory applications. [2013-0109]**

***Index Terms*—Nanoelectromechanical systems, relay, switch, van der Waals, nonvolatile memory, Bistable, electrostatic.**

I. Introduction

The ever quest in CMOS scaling has expanded the exploration boundary beyond conventional transistor, listing from quantum devices, ultrathin body silicon on insulator (SOI), fin-FET, and so on. Most devices leverage on the transportation of electrons or the same to determine the on–off criteria [1], [2]. Until recently, nanoelectromechanical (NEM) relay has drawn great attention due to its exceptional properties. NEM relay is a physically actuated nanoscale mechanical switch that does not rely on transportation or storage of charges. Instead, NEM relay relies on mechanical switching motion and geometrical shape to replicate logic operation in transistor and solid state nonvolatile memory (NVM) and its advantages include extremely low off-state leakage current, steep sub-threshold slopes, and capability of high temperature operation [3]–[5]. It is already reported that the NEMS relay can complement CMOS circuits resulting in faster operation and erasing speed [6], [7]. Besides that, reports suggest that the NEM switches can overcome poor performance usually at the extremes of temperature because of their mechanical switching nature [8]. Here, we propose a NVM that demonstrates hysteresis behavior under the influence of van der Waals force (VDW).

Manuscript received April 11, 2013; revised May 12, 2013; accepted June 2, 2013. Date of publication July 3, 2013; date of current version September 27, 2013. This work was supported by the SERC of the Agency for Science, Technology and Research under Grant 1021010022. Subject Editor H. Fujita.

B. Soon and Y. Qian are with the Institute of Microelectronics, Agency for Science, Technology and Research, Singapore 117685, and also with the Department of Electrical and Computer Engineering, National University of Singapore, Singapore 117576.

E. J. Ng is with the Department of Mechanical Engineering, Stanford University, Stanford, CA 94305 USA.

N. Singh is with the Institute of Microelectronics, Agency for Science, Technology and Research, Singapore 117685.

J. M. Tsai is with Advanced Technology, InvenSense, Inc. Sunnyvale, CA 94089 USA.

C. Lee is with the Department of Electrical and Computer Engineering, National University of Singapore, Singapore 117576 (e-mail: elelc@nus.edu.sg).

Color versions of one or more of the figures in this paper are available online at http://ieeexplore.ieee.org.

Digital Object Identifier 10.1109/JMEMS.2013.2266859

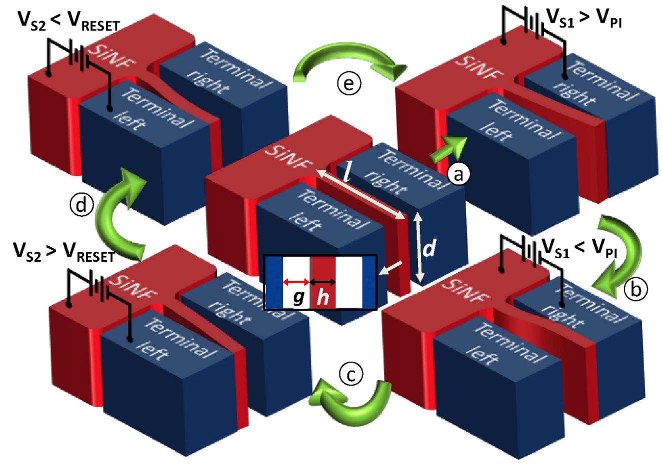

Fig. 1. Structure and operation of a bistable NEM relay. (a) SiNF is pulled-in to the right terminal by V_{S1}. (b) VDW force will hold the SiNF in contact position even after the electrostatic force is removed. (c) When an opposite bias is applied, SiNF flips toward the other terminal. (d) VDW force holds the switch in left terminal. (e) Switch cycles between two terminals, resulting in bistable state device.

II. Device Concept and Operation

The operating concept and device structure is illustrated in Fig. 1. A high aspect ratio (1:35) silicon nanofin (SiNF) is fabricated using entirely CMOS process. The dimension of the SiNF consists of 2-, 8-, and 12-μm length (l) with 80-nm thick (h) and 3.5-μm height (d). The gap (g) between the SiNF to either terminal is approximately 80 nm. The SiNF is designed to switch between two-side lateral terminals by electrostatic force. In contrast to the previous work [9], this reported switch is lateral based, lower pull-in voltage (V_{PI}) and its cyclic behavior is clearly demonstrated. Initially, the SiNF is in a neutral state. SiNF is pulled in to the right terminal when a sweeping voltage (V_S) is applied across SiNF and right terminal at initial sweeping voltage > pull-in voltage ($V_{S1} > V_{PI}$). Subsequently, when this voltage is removed, VDW attraction at the interface between SiNF and electrode will maintain the contact without on-hold bias, resulting in hysteresis behavior.

Meanwhile, The SiNF flips and switches toward the opposite lateral terminal when a second sweeping voltage (V_{S2}) is applied across the left terminal. In this report, the SiNF structure makes NEM relay switch bidirectionally while exhibiting bistability, thus it is able to provide two different states. Both stable states available attributed to VDW force enable the NEM relay to serve as storage layer-free NVM.

III. Experiment Result and Discussion

NEM relay has been fabricated using CMOS facility and systematically characterized. First, SiNF is defined on SOI

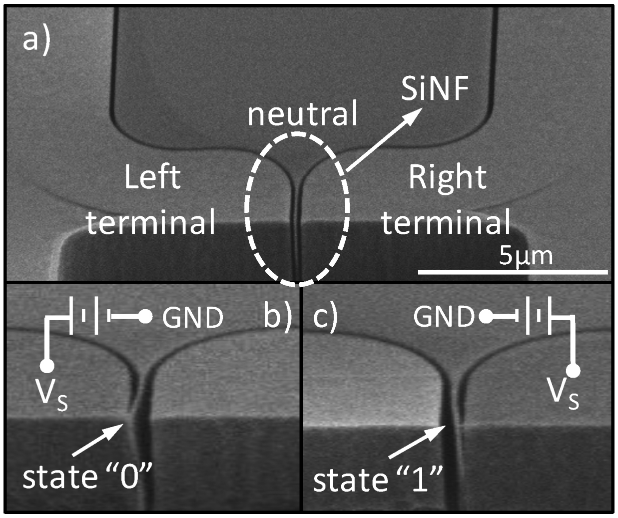

Fig. 2. SEM photo showing a 2-μm length $\times$ 80-nm width SiNF in operation. (a) SiNF remains at neutral position. (b) SiNF contact remains on-hold to the left terminal, depicting state "0." (c) SiNF flips to the right terminal and on-hold to the right terminal, depicting state "1."

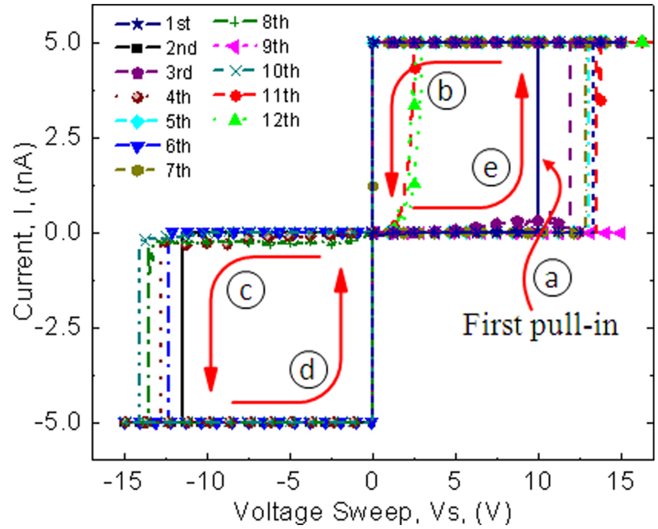

Fig. 3. Measured I_S–V_S curve of 2 μm $\times$ 80 nm SiNF showing bistable hysteresis of the device. (a) Initial pull-in to the right terminal. (b) Left terminal contact on-hold by the VDW. (c) SiNF flips to the left terminal. (d) Right terminal contact on-hold by the VDW. (e) SiNF pull-in to the right terminal.

wafers with 3.5 μm device layer and 1 μm BOX. Silicon is chosen as the starting material to be implemented due to its compatibility in nanoscale microfabrication processing, the structure consists of single crystal Si and will be stress-free upon release, forming a completely straight beam. Dry oxidation 1100°C in O_2 flow is further performed to reduce the SiNF dimension to the desired value of 80 nm. The etched surface of the SiNF is also smoothened in this process to enhance the surface forces so that it adheres to the terminal electrode when in contact. The device layer is heavily implanted twice by arsenic with a dosage of 5×10^{15} ions/cm^2, and activated in order to make the SiNF as conductive as possible, the impurity concentration at 2.0 μm is approximately 1.0×10^{15} ions/cm^2. Dry release of vapor hydrofluoric (VHF) acid is used in the last process to suspend the SiNF while preventing stiction problem. In real application, the SiNF fabrication has to be processed first before CMOS fabrication due to high temperature oxidation. Fig. 2(a) shows the SEM diagram of a 2 μm $\times$ 80 nm NEM relay in a neutral state. Fig. 2(b) and (c) show the SEM diagram of an actuated SiNF through sweeping voltage applied across SiNF and either terminal. Note that the charging difference in the SEM showing the connection difference when the SiNF is in contact with either terminal. The 2-μm device's contact edge to the actuating terminal is minimal at edge. The device inspected in SEM is electrically tested and we found that remains in contact and the direction agree well with where voltage is previously applied.

In electrical test, a voltage sweep (V_S) is applied across left terminal and right terminal from negative region (0 to - 15 V) to positive region (0 to 15 V) under N_2 purged microchamber (CASCADE RBL6100) at elevated temperature of 50°C to remove any moisture. Hence, we assume that capillary force is negligible. The corresponding cyclic behavior of a 2-μm length by 80-nm width SiNF is shown in Fig. 3. The pull-in phenomenon is represented by an abrupt increase in sweeping current (I_S), usually between two voltage steps. The first pull-in is considered as the SiNF is at neutral position, this pull-in voltage is usually lower due to smaller initial gap. When sweeping voltage is less than pull-in voltage ($V_S < V_{PI}$), continuous flow of sweeping current (I_S) shows that the relay maintains its contact with the lateral terminal by surface force, since there is no sign of SiNF pull-out and electrostatic force is lower than spring restoration force. At 0 V, sweeping current returns to near fA range as there is no voltage applied by the analyzer. As sweeping voltage reversed from 0 to - 15 V across left terminal, SiNF flips, and pull-in to the left terminal at around 11.5 V. The pull-in voltage after the first pull-in is higher but does not scale according to pull-in model, this is due to the nonuniform gap size. To program or erase the device, a pull-in voltage needs to be applied across the SiNF and the terminal. Meanwhile, read operation can be performed by low current measurement where already switched SiNF are subjected to a read potential much less than the pull-in voltage ($V_{read} < V_{PI}$) in order to sense the current ($V_{read} < V_{PI}$).

The switch continues to operate until the 11th sweep before no pull-in is observed, we found sweeping current returns zero at 2 V, resembling a charging curve during the reverse sweep. A repeated 12th sweep shows this current follows the charging curve and no pull-in can be detected anymore, depicting that the switch has failed. Observation under SEM shows that the switch is melted, as the SiNF is fused to the right terminal.

The abrupt jump in sweeping current corresponds to on–off current ratio (I_{on}/I_{off}) of 10^2 which is considered far from ideal due to the compliance current setting of 5 nA. Low current compliance prevents excessive current from flowing through SiNF where the excessive current may cause device failure due to fusing and oxidation of Si. Thus, the device suffers from poor yield and reliability. This may improve if the testing is done under vacuum encapsulation which is viable at packaging level and may prove valuable to such devices [10]. Other alternative solution like contact enhance coating like Au, Pt, and RuO_2 may solve this issue but the fabrication of such small device will be extremely challenging [11], [12]. The on–off current ratio of 10^5 is demonstrated

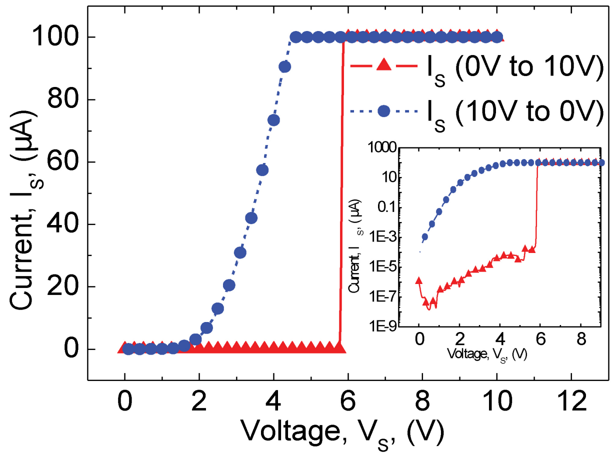

Fig. 4. Measured I_S–V_S curve of an 8-μm length SiNF device. The current compliance of the measurement is limited up to 100 μA. From 0 to 10 V, measured V_{PI} is 5.95 V at 25 mV/decade. The measured I_{ON}/I_{OFF} is 10^5. From 10 to 0 V, the pull-out is not abrupt but shows charging relation.

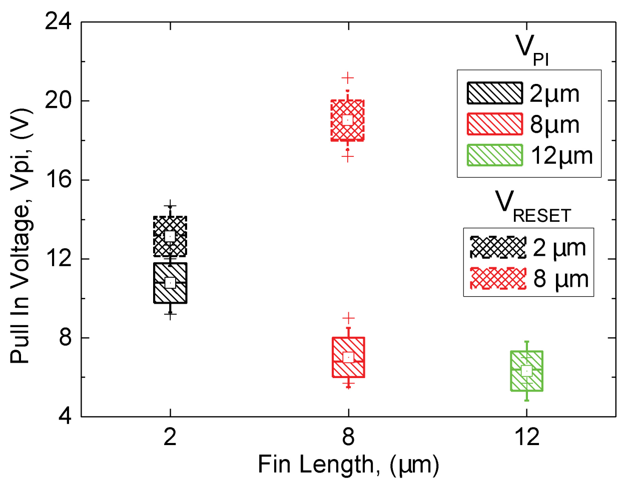

Fig. 5. Constant error bar of V_{PI} and V_{RESET} versus 2-, 8-, and 12-μm long SiNF of 20 devices. V_{PI} reduced while V_{RESET} increases sharply, while device with fin length of 12 μm cannot be reset due to permanent adhesion.

with 100-μA current compliance as shown in Fig. 4 with the similar device, but the device works for only once. This is shown from when the sweeping current gradually reduce when sweeping voltage is decreasing, resembling current discharging curve, which may be caused by SiNF melted to the respective actuating terminal. To further confirm this, SEM inspection is performed for the same device tested and we confirmed that the SiNF is melted to the terminal under high operating current. The pull-in voltage is 5.95 V at 25 mV/decade, achieving five-order of on–off ratio. From the experimental results, we show that the length is crucial in designing a resettable switch. Fig. 5 shows the correlation between the pull-in voltage (V_{PI}) and reset voltage (V_{RESET}) versus the length of the SiNF. The measurement is performed statistically for 20 devices and results show that pull-in voltage is inversely proportional to SiNFs length. The experimental pull-in voltage is found to be higher than the expected value from analytical model [13], possibly due to fabrication tolerance especially in the release process and nonuniform electrostatic force. However, the resetting voltage is agreeable to the finite element analysis performed in ANSYS simulation. The nonvolatile hysteresis behavior is only obtainable in 2-and 8-μm devices. Overwhelming adhesion force causes a drastic increase in resetting voltage as the SiNF length increases in 8-μm SiNF, and, eventually, leads to permanent adhesion in 12-μm SiNF relay. The trade-off between the required pull-out energy and the VDW force has to be taken into design consideration.

Nonetheless, the operating voltages demonstrated are far from ideal, one possible solution is probably applying torsion configuration to further reduce the spring constant of the SiNF, and, hence, to achieve reduction in pull-in voltage while keeping the device nanoscale footprint [14]. Do note that after the initial SiNF pull-in, the resetting voltage will be the operating voltage for write and erase in NVM application.

IV. Conclusion

In summary, a lateral high aspect ratio and NEM relay is fabricated and characterized. The switch is capable of providing bistable states and therefore it operated as NVM. Meanwhile, the nanosized gap and width of the SiNF made the device attractive for scalability with estimated compact density about 390 kb/mm^2.

References

[1] K. K. Likharev, "Single-electron devices and their applications," *Proc. IEEE*, vol. 87, no. 4, pp. 606–632, Apr. 1999.

[2] G. Tsutsui, M. Saitoh, and T. Hiramoto, "Experimental study on superior mobility in (110)-oriented UTB SOI pMOSFETs," *IEEE Electron. Device Lett.*, vol. 26, no. 11, pp. 836–838, Nov. 2005.

[3] J. Jaeseok, V. Pott, H. Kam, R. Nathanael, E. Alon, and T. K. Liu, "Seesaw relay logic and memory circuits," *J. Microelectromech. Syst.*, vol. 19, no. 4, pp. 1012–1014, Aug. 2010.

[4] S. Chong, B. Lee, K. B. Parizi, J. Provine, S. Mitra, R. T. Howe, and H. P. Wong, "Integration of nanoelectromechanical (NEM) relays with silicon CMOS with functional CMOS-NEM circuit," in *IEDM Tech. Dig.*, Dec. 2011, pp. 30.5.1–30.5.4

[5] K. Akarvardar and H. S. Wong, "Ultralow voltage crossbar nonvolatile memory based on energy-reversible NEM switches," *IEEE Electron. Device Lett.*, vol. 30, no. 6, pp. 626–628, Jun. 2009.

[6] S. Chong, B. Lee, S. Mitra, R. T. Howe, and H. P. Wong, "Integration of nanoelectromechanical relays with silicon nMOS," *IEEE Trans. Electron. Devices*, vol. 59, no. 1, pp. 255–258, Jan. 2012.

[7] S. W. Lee, S. J. Park, E. E. B. Campbell, and D. Chen, "A fast and low-power microelectromechanical system-based nonvolatile memory device," *Nature Commun.*, vol. 2, no. 220, pp. 1–6, Mar. 2011.

[8] T. H. Lee, S. Bhunia, and M. Mehregany, "Electromechanical computing at 500 C with silicon carbide," *Science*, vol. 329, pp. 1316–1318, Sep. 2010.

[9] V. X. H. Leong, E. J. Ng, J. B. W. Soon, N. Singh, N. Shen, T. Myint, V. Pott, and J. M. Tsai, "Vertical silicon nano-pillar for non-volatile memory," in *Proc. IEEE Transducers*, Jun. 2011, pp. 649–652.

[10] D. A. Czaplewski, C. Nordquist, C. Dyck, G. Patrizi, G. Kraus, and W. D. Cowan, "Lifetime limitations of Ohmic, contacting RF MEMS switches with Au, Pt And Ir contact materials due to accumulation of 'friction polymer' on the contacts," *J. Micromech. Microeng.*, vol. 22, no. 10, pp. 1–12, Aug. 2012.

[11] R. Parsa, M. Shavezipur, W. S. Lee, S. Chong, D. Lee, H. P. Wong, R. Maboudian, and R. T. Howe, "Nanoelectromechanical relays with decoupled electrode and suspension," in *Proc. IEEE MEMS*, Jan. 2011, pp. 1361–1364.

[12] D. A. Czaplewski, C. Nordquist, G. Patrizi, G. Kraus, and W. D. Cowan, "RF MEMS switches with RuO_2–Au contacts cycled to 10 billion cycles," *J. Microelectromech. Syst.*, vol. 22, no. 3, pp. 655–661, Jun. 2013.

[13] O. Y. Loh and H. D. Espinosa, "Nanoelectromechanical contact switches," *Nature Nanotech.*, vol. 7, no. 5, pp. 283–295, 2012.

[14] W. Xiang and C. Lee, "Nanoelectromechanical torsion switch of low operation voltage for nonvolatile memory application," *Appl. Phys. Lett.*, vol. 96, no. 19, pp. 1–3, 2010.